

## Brachiola vesicularum, N. G., N. Sp., a New Microsporidium Associated with AIDS and Myositis

ANN CALI,<sup>1,2</sup> PETER M. TAKVORIAN,<sup>3</sup> SHARON LEWIN,<sup>2</sup> MICHAEL RENDEL,<sup>2</sup> CORAZON S. SIAN,<sup>2\*</sup> MURRAY WITTNER,<sup>4,5</sup> HERBERT B. TANOWITZ,<sup>4,5</sup> ELAINE KEOHANE<sup>4,5,6</sup> and LOUIS M. WEISS<sup>4,5</sup>

<sup>1</sup>Department of Biological Sciences, 101 Warren Street, Smith Hall, Rutgers University, Newark, New Jersey 07102, USA, and

<sup>2</sup>Saint Luke's Roosevelt Hospital Center, 1111 Amsterdam Avenue, New York, New York 10025, USA, and

<sup>3</sup>Department of Pathology, Division of Parasitology, Albert Einstein College of Medicine, Bronx, New York 10461, USA, and

<sup>4</sup>Department of Clinical Laboratory Sciences, University of Medicine and Dentistry of New Jersey, Newark, New Jersey 07107, USA

**ABSTRACT.** *Brachiola vesicularum*, n. g., n. sp., is a new microsporidium associated with AIDS and myositis. Biopsied muscle tissue, examined by light and electron microscopy, revealed the presence of organisms developing in direct contact with muscle cell cytoplasm and fibers. No other tissue types were infected. All parasite stages contain diplokaryotic nuclei and all cell division is by binary fission. Sporogony is disporoblastic, producing  $2.9 \times 2 \mu\text{m}$  diplokaryotic spores containing 8–10 coils of the polar filament arranged in one to three rows, usually two. Additionally, this microsporidium produces electron-dense extracellular secretions and vesiculotubular appendages similar to *Nosema algerae*. However, the production of protoplasmic extensions which may branch and terminate in extensive vesiculotubular structures is unique to this parasite. Additionally, unlike *Nosema algerae*, its development occurred at warm blooded host temperature ( $37$ – $38^\circ\text{C}$ ) and unlike *Nosema connori*, which disseminates to all tissue types, *B. vesicularum* infected only muscle cells. Thus, a new genus and species is proposed. Because of the similarities with the genus *Nosema*, this new genus is placed in the family Nosematidae. Successful clearing of this infection (both clinically and histologically) resulted from treatment with albendazole and itraconazole.

**Supplementary key words.** Appendages, microspora, microsporidiosis, morphogenesis, muscle tissue, nosematidae, protoplasmic extensions, taxonomy, tubules, vesiculotubular structures.

SEVEN genera and several species of microsporidia infecting humans (phylum, Microspora) have been reported. Most of these infections are in association with AIDS. These genera are *Nosema* [14], *Enterocytozoon* [10], *Pleistophora* [13], *Encephalitozoon* [25], *Septata* [6], *Vittaforma* [18], and *Trachipleistophora* [11]. Three of them have been described in muscle tissue: *Pleistophora* sp., *Trachipleistophora hominis*, and *Nosema connori*. *Pleistophora* sp. [9, 13] and *Trachipleistophora hominis* [11] infections were demonstrated in skeletal muscle in association with immune incompetence and myositis. Both of these parasites form sporophorous vesicles, in which parasite development occurs. They are both polysporous and possess unpaired nuclei in all stages of development. *Nosema connori* was reported from an athymic infant with severe malabsorption diarrhea. Histological examination of autopsy tissues revealed microsporidiosis had disseminated to most of the tissues sampled, including muscle cells of the diaphragm and intestine [14, 16, 20, 22]. Recently, Trammer et al. [26] injected athymic mice with *N. algerae* and reported disseminated infection in the tail and foot pads. A comparison of these two organisms with the new parasite is provided.

Based on our initial histological observations of a parasite with diplokaryotic nuclei, developing in direct contact with muscle cell cytoplasm, the parasite was described as *Nosema*-like when presented at the IVth International Workshop on Opportunistic Protists in Arizona and published in its proceedings (Cali, A., Takvorian, P. M., Lewin, S., Rendel, M., Sian, C., Wittner, M., & Weiss, L. 1996. Identification of a new microsporidian associated with AIDS and myositis. Abstract. *J. Euk. Microbiol.*, 43:108S). However, unlike *Nosema* or any of the above mentioned microsporidia, this organism has a unique

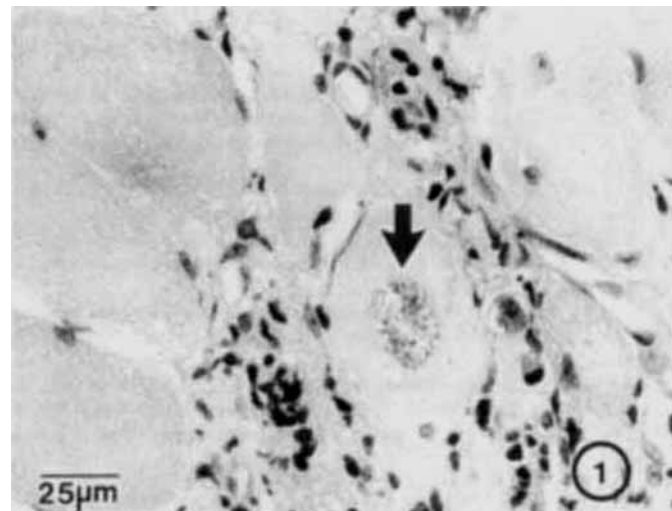


Fig. 1. H & E stained section of left quadriceps muscle biopsy from a patient with microsporidian myositis. A mononuclear infiltrate is present, consistent with granulomatous myositis. The arrow head indicates the infected myocytes (myofibers) and demonstrates cytolysis in the presence of the organism. The spores are approximately  $2.5 \mu\text{m}$  in size. No organisms are present in the interstitial connective tissue or inflammatory cells.

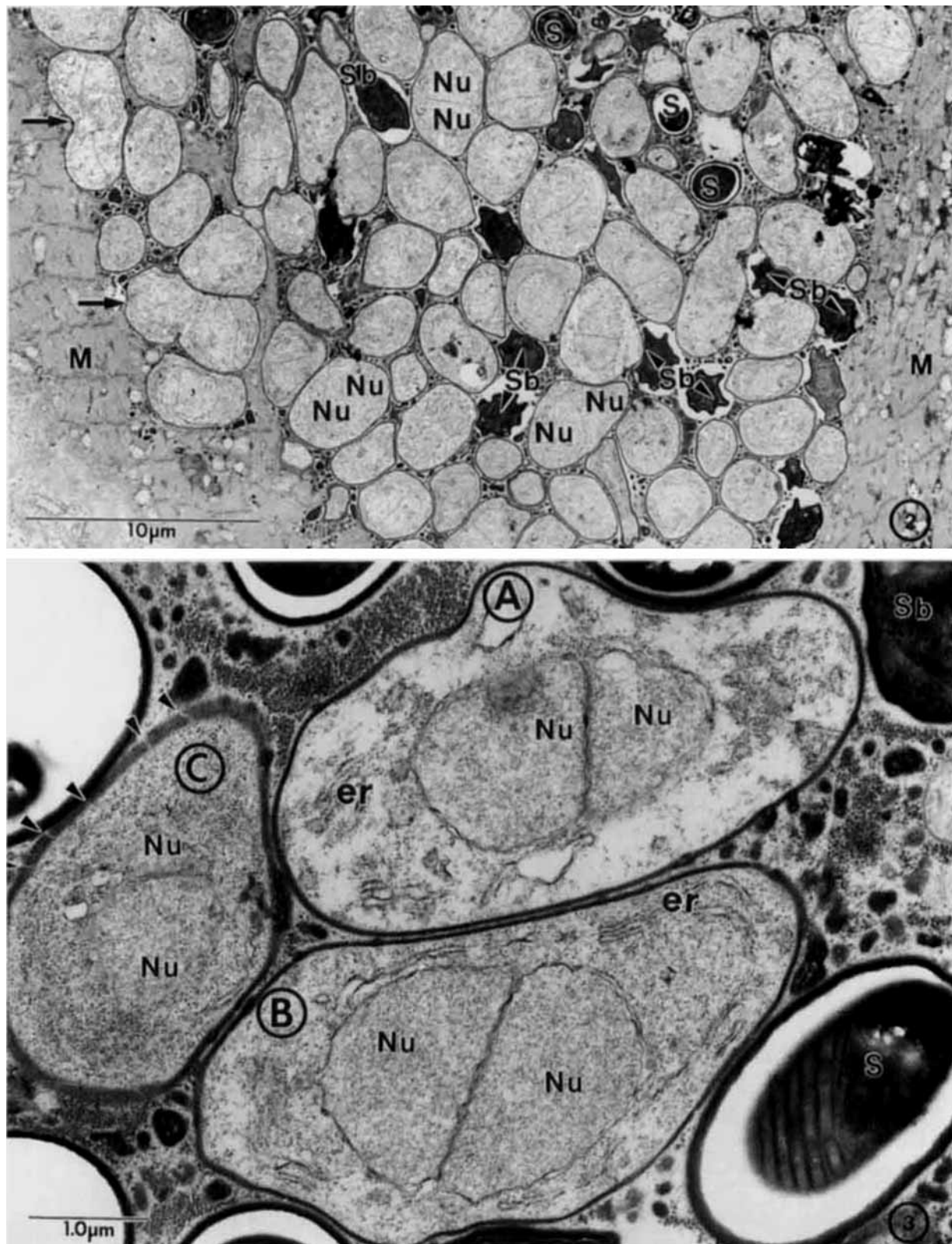
combination of features resulting in the need for a new generic designation.

### MATERIALS AND METHODS

A 31 year old white male serologically positive for HIV with a CD4 count of  $35/\text{mm}^3$  and fever ( $38^\circ\text{C}$ ) had progressive muscular weakness of the lower extremities with pain for five

\* To whom correspondence should be addressed. Telephone: 973-353-5364; Fax: 973-353-1007.

Fig. 2–3. Electron microscopic overview of an infected muscle cell. 2. Developmental stages of the parasite appear as clusters surrounded by the striated muscle cell filaments (M). The electron-density variations of the parasite cells are readily observable, they represent different stages of parasite development, the most dense stages are sporoblasts (Sb) and spores (S). Diplokaryotic nucleation (Nu) is apparent in the majority of parasitic cells. Some dividing cells contain two diplokarya (arrows). 3. Higher magnification of several parasite cells illustrating the variation in



electron-density and the presence of diplokaryotic nuclei (Nu). More subtle differences can also be observed in the earlier stages of parasite development. Two of the proliferative cells (A and B) are covered by a uniform coat (40–50 nm) of electron-dense material that appears to be continuous with the plasmalemma. Each cell contains a well-defined diplokaryon, however, the cytoplasm of these cells varies considerably. Cell A appears less electron-dense because the cytoplasm is less granular. It has few ribosomes and scant amounts of rough endoplasmic reticulum (er) as compared to cell B. The cytoplasm of a third cell (C) contains large amounts of granular material and is also limited by a thick coat of electron-dense material. The thick coat has several narrow electron-lucent channels traversing it (arrow heads). Note the presence of the more electron-dense sporoblast (Sb) and spore (S).

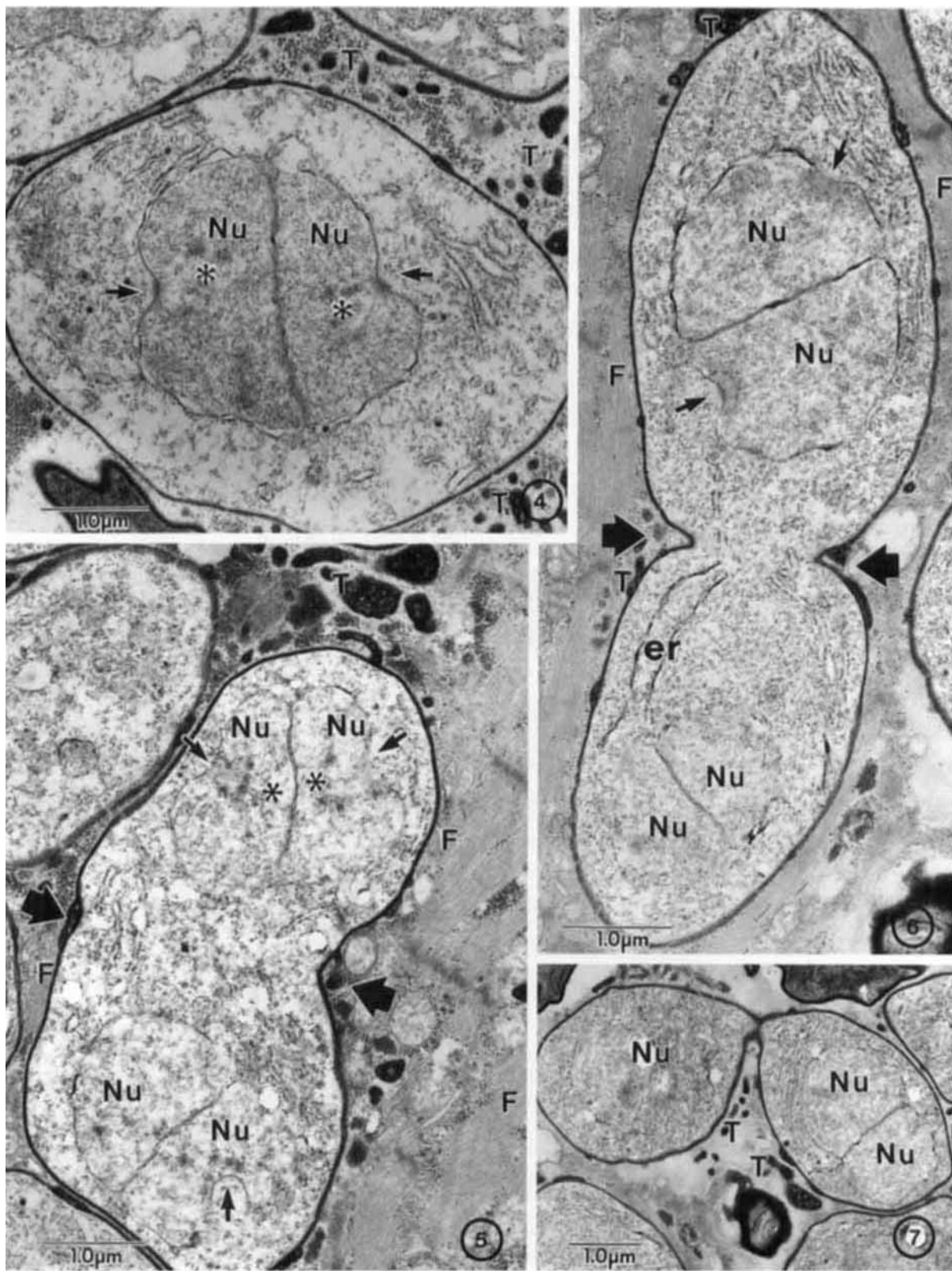


**Fig. 4-7.** Karyokinesis and cytokinesis. **4.** Early proliferative cell with diplokaryotic nuclear (Nu) pair undergoing karyokinesis. Nuclear membrane invaginations containing spindle plaques on each nuclear envelope (arrows) of the diplokaryotic pair and chromosomes (\*) within each respective nucleoplasm are present. Note the presence of vesiculotubular material (T) in the host cytoplasm. **5.** Early proliferative cell containing two diplokaryotic nuclear pairs, both with nuclei in late anaphase. Note chromosomes (\*) in close association with spindle plaque (arrow). Plasmalemmal invagination (broad arrowheads) indicating cytokinesis has commenced, prior to the nuclei entering interphase, thus linking the two processes. The parasite cells are in direct contact with the muscle cell cytoplasm with no intervening parasitophorous vacuole as evidenced by the proximity of the myofilaments (F). **6.** A proliferative cell in a more advanced stage of cytokinesis (broad arrowheads) and the spindle

months. The left quadriceps muscle was biopsied for culture (bacterial, fungal and mycobacterial) and histology. The biopsy tissue for both light and electron microscopy, was fixed in McDowell commercially prepared fixative (Poly Scientific). The wax embedded sections were hematoxylin and eosin (H & E) stained and the semi-thin plastic sections were stained with 1% toluidine blue. Thin sections were stained with aqueous uranyl acetate and lead citrate, and observed with a Philips CM-10 TEM at the Rutgers University, Newark, Electron Microscope Facility.

**Polymerase chain reaction (PCR).** The *Nosema algerae* ribosomal RNA large subunit partial sequence (L28961) [3] was used to design two primers NAG6f (5'GCCGTTTCGAAGTT GG3') and NAG 178r (5'ATATCGACGGGACTCTCAC3') which produce a 192-bp amplicon from *Nosema algerae*. Muscle biopsy material and formalin fixed *Nosema algerae* spores (purified from in vitro culture in RK-13 cells at 28°C) were extracted using TaDaRa DexPAT (Takara BioMedicals). Briefly, spores or two 5 µm thick paraffin embedded tissue sections were mixed with 0.5 ml of DEXPAT reagent, heated to 100°C for 10 min and centrifuged at 16,000 g for 10 min at 4°C. The supernatant was removed and 1 to 10 µl was used for PCR. The PCR was performed in a 100 µl reaction on a Perkin Elmer 2400 PCR machine using standard buffer conditions (1X PCR buffer, 2.0 mM MgCl<sub>2</sub>, 0.4 µM of each primer) employing 2.5 U of AmpliTaq Gold (Perkin Elmer Cetus-Applied Biosystems, Foster City, CA). The PCR reaction was carried out at: 95°C for 7 min followed by 35 cycles of 95°C for 1 min, 48 to 55°C for 1 min and 72°C for 1 min and then completed by incubation at 72°C for 7 min.

A type slide has been deposited with the International Protozoan Type slide collection (#50968) in the National Museum of Natural History.

## RESULTS

**Light microscopy and clinical course.** Cultures for bacteria, fungi, and mycobacteria were negative. Clusters of organisms were visible within the muscle cells of muscle biopsy tissue by light microscopy of the H & E stained wax embedded tissue (Fig. 1). Histologic examination reveals granulomatous myositis. As can be seen in this figure, there is a predominately mononuclear cell infiltration in the interstitium between the muscle fibers. Within H&E stained muscle fibers, areas of myolysis (cytolysis) were evident and within these areas numerous developing stages and spores were observed. The spores measured 2 × 2.5 µm. No organisms were present within the interstitium or in inflammatory cells.

The patient was empirically treated with pyrimethamine and sulfadiazine for presumed *Toxoplasma gondii* myositis without improvement. On review of the biopsy the diagnosis of microsporidiosis was suggested and a second biopsy was performed and examined by light and electron microscopy. The diagnosis of a microsporidian infection was confirmed by electron microscopy and the patient was started on albendazole 400 mg twice daily (BID). On this, the patient improved with an increase in muscle strength and resolution of fever. Itraconazole 400 mg once daily (QD) was added one month later and his symptoms continued to improve. A third muscle biopsy demonstrated that the organisms were no longer seen and the in-

flammatory response had resolved histologically. The patient returned to a normal muscle strength and functioning until several months later when he developed a viral pneumonitis and expired.

**Transmission electron microscopy (TEM).** Within the muscle cells, clusters of parasites appear in direct contact with the myofilaments and other host cell organelles (Fig. 2). The clusters consist of mostly diplokaryotic cells, with some dividing cells containing two diplokarya. The spores and sporoblasts are the most obvious as they are electron-dense and contain the polar filament (Fig. 2). The remaining stages are more difficult to differentiate from each other as they all possess a thick plasmalemma. However, these cells vary in cytoplasmic density and complexity. The least electron-dense cells (Fig. 3) have a simple finely granular cytoplasm with few granules and short segments of rough endoplasmic reticulum (ER). Other cells are more electron-dense, containing more cytoplasmic granules and ER (Fig. 3). It appears that increasing density is a continuous process because cells intermediate between these are also present.

All stages contain diplokaryotic nuclei. The nuclei making up the diplokaryotic pair are often seen in the process of division, yet the cells have not been observed with more than two diplokarya in them (Fig. 3–7). The observation of dividing nuclei in the dividing cells indicates that cytokinesis commences before karyokinesis is completed (Fig. 5–7), demonstrating that in this microsporidian, the two processes are linked. These proliferative cells are oval to elongated (Fig. 4–7) with the nuclei occupying the vast majority of the cell's contents. No multinucleate plasmodia or long ribbon-like stages containing more than two diplokarya occur. The sporonts are not clearly differentiated as all cells have a thick, electron-dense coating on the plasmalemma. Since all cell division is by simple binary fission, it is reasonable to assume this organism is disporoblastic.

The sporoblasts are discernible even when the developing polar filament is not yet present because of their extremely dense cytoplasm and crenated shape presenting a condensed appearance (Fig. 8) as opposed to the less-dense generally oval earlier stages (Fig. 3). Additionally, after the last cell division these sporoblasts each contain a diplokaryon and as polar filament formation commences, its associated structures appear. Their plasmalemmal coat of electron-dense material is thicker (45–65 nm) and more dense than the coating on proliferative stages (28–35 nm). This thickening layer will become the exospore (outer) coat of the spore.

After the polar filament development is well established the electron-lucent endospore coat becomes visible (Fig. 9). It first appears as a thin band between the plasmalemma and immediately inside the thick electron-dense exospore coat. It becomes progressively thicker as spore maturation continues, resulting in an endospore that is many times thicker than the exospore. It should be noted that in late sporoblasts the polar filament coils were observed in single (Fig. 9) and double rows (Fig. 10).

Inside the spores, the polar filament forms 7–10 coils (typically 9) usually in a double row (Fig. 11), however, they have also been observed containing a triple row of coils in a cluster or as a single row (Fig. 12, 13). The polar filament is anisofilar;

←

plaques (arrows) are still present. The cytoplasm of this proliferative cell is more densely granular and endoplasmic reticulum (er) is more abundant than in the previous two cells indicating that this cell is also more advanced in the parasite developmental cycle. Note the presence of myofilaments (F) and of vesiculotubular material (T). 7. A late proliferative/sporont cell completing cytokinesis. The plasmalemmal invagination is almost complete and the diplokaryotic nuclear (Nu) pairs appear to be in interphase. Note the presence of vesiculotubular material (T).

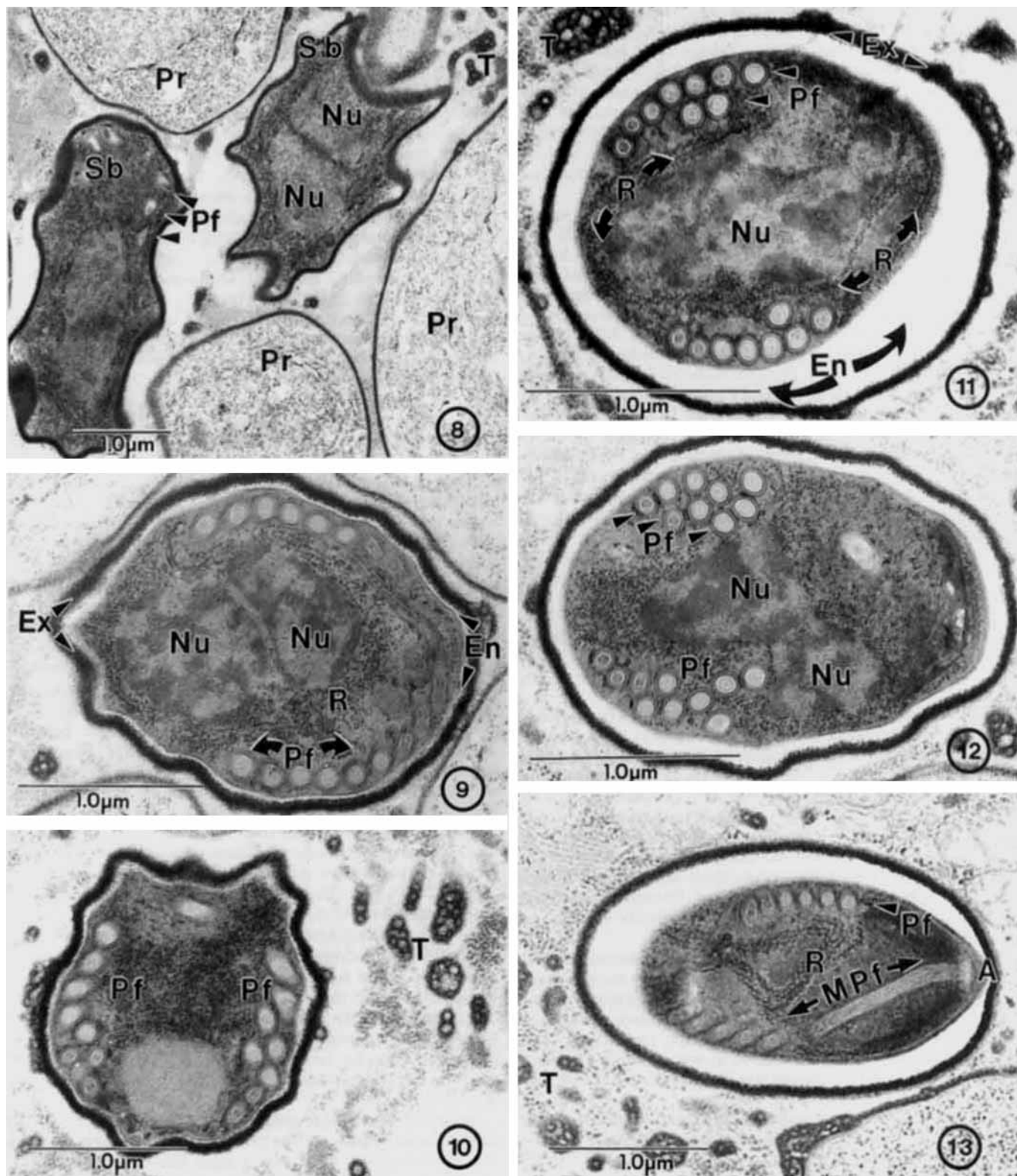


Fig. 8-13. Spore morphogenesis. **8.** Two sporoblasts (Sb) discernible because of their extremely dense cytoplasm, crenated shape, and lack of an electron-lucent endospore wall. Note the lighter staining of the proliferative cells (Pr) in this figure. The plasmalemmal coat of electron-dense material is thicker (45–65 nm) and more dense than the coating on proliferative stages (28–35 nm). Diplokaryotic nuclei (Nu) are present in both sporoblasts and cross sections of the developing polar filament (Pf) can be seen in one. A cluster of vesiculotubular material (T) appears to be attached to one of the sporoblasts. **9.** Sporoblast. The thickened plasmalemmal secretions (62–80 nm) will become the exospore coat (Ex) when the electron-lucent endospore region (En) becomes visible as a thin ring (16–40 nm) surrounding the sporoplasm and immediately adjacent to the thin plasmalemmal membrane. The sporoplasm contains approximately eight polar filament (Pf) cross sections arranged in a single row near the periphery. The diplokaryotic nuclei (Nu) are centrally located and are encircled by arrays of ribosomes (R). **10.** Sporoblast. The electron-

the anterior most coils being of larger diameter (~123 nm) than the posterior most two to three coils (~112 nm) which appear to taper slightly (Fig. 11, 12). Longitudinal sections of the spores reveal the presence of an anterior polar filament anchoring disc complex with a lamellar polaroplast extending laterally to the periphery of the spores while the tubular polaroplast is more centrally located. The sporoplasm contains the diplokaryotic nuclei which are surrounded by copious arrays of ribosomes filling the area between the nuclei and the polar filament (Fig. 11, 13). The spore size ranges from  $2.5-2.9 \times 1.9-2.0 \mu\text{m}$  in fixed material but is typically  $2.9 \times 2.0 \mu\text{m}$ . Parasite development is asynchronous in this microsporidian, because the various developmental stages are scattered irregularly among each other (Fig. 2).

**Extracellular secretions and appendages.** The surface of the parasite plasmalemma is extremely diverse. It is covered with extracellular secretions that appear as electron-dense material. This material varies in its thickness, investments, and morphological appearance along the parasite cell surface and as parasite development proceeds it is present in some form on all stages (Fig. 14, 15). Higher magnification of the extracellular material reveals the presence of several distinct morphological entities. Around the cell surface is the electron-dense material which often appears fibrous (Fig. 16) with discontinuities or gaps which extend down to the plasmalemma occurring irregularly. In some stages it appears to have electron-lucent "blisters" that occur regularly and continuously around large portions of the cell (Fig. 17). When cut tangentially, this type of cell surface appears ridged or as alternating regular dark and light banding (Fig. 15, 17). A second type of ridges or banding has uniform sized electron-lucent "channels" with irregular and much larger areas of electron-dense material (Fig. 3) similar to the "scalloped" surface of many microsporidia as they begin sporogony.

**Appendages.** There are electron-lucent spherical vesicles (Fig. 18–20) and/or tubules (Fig. 21, 22) with dilations and constrictions (vesiculotubular structures) that appear very irregularly along the cell surface. The vesiculotubular structures appear to be embedded in or surrounded by the electron-dense material. On some cell surface areas these structures occur parallel to the cell surface (Fig. 18, 20) and on others there are irregular large accumulations of the fibrous and vesicular material protruding off small areas of the cell surface (Fig. 22–24). In the areas between the developing parasite cells, much of this electron-dense vesicular material is present (Fig. 23, 24). It can be present as large clusters of irregularly arranged vesicles to long single strands of vesicles, similar to a strand of beads (Fig. 23). These strands may become quite long (over  $0.85 \mu\text{m}$ ). Sometimes, after cell division has occurred, the vesiculotubular material remains continuous between the two cells (Fig. 24). During sporogenesis some remnants of vesiculotubular structures on the exospore coat may be present. While vesiculotubular structures are present in the host tissue immediately surrounding the spores, relatively little of this material

appears to remain attached to the exospore coat of the mature spores (Fig. 11–13).

**Protoplasmic extensions.** The appendages may occur as vesiculotubular structures surrounded by electron-dense material on the parasite plasmalemma surface as above, or attached to elongated, sometimes branched protoplasmic extensions. The protoplasmic extensions are projections that are continuous with the parasite cell cytoplasm, not structures attached to, or on the surface of, the cell. Some developing parasite cells, having the general characteristics of proliferative forms, elongate without undergoing further karyokinesis and have vesiculotubular complexes associated with the end or ends of these elongating cells (Fig. 25, 26). It is this type of cell that produces the protoplasmic extensions. These extensions branch and terminate with attached electron-dense vesiculotubular structures. Variations occur in the appearance of these protoplasmic extensions and the vesiculotubular complexes associated with them (Fig. 27–29). Once sensitized to the appearance of these structures, they can be observed in many of the micrographs.

**Host cell pathology.** The parasite appears limited to the cytoplasm of skeletal muscle cells. No infection was observed by histological examination (at both the light and EM level) of all other tissue types in the vicinity of infected muscle. Only remnants of spores were observed in some phagocytic cells.

Within the infected muscle cells, the parasites are in direct contact with the host cell cytoplasm. Appendages, vesiculotubular complexes with or without protoplasmic extensions, appear as variously shaped electron-dense masses and are abundant in the surrounding host cell cytoplasm. The host cell organelles (myofibrils and mitochondria) are present and intact around the periphery of the parasite cluster (Fig. 2) and abutting individual parasite cells with few to no visible appendages (Fig. 5). However, host organelles are not present in areas where the appendages are in abundance (Fig. 3, 4). It should be noted that this is not due to a general host cell necrosis. Rather, the lack of host cell organelles appears to be extremely localized to the specific areas of parasite appendages (Fig. 5). One side of a parasite cell may have multiple appendages next to it and no host organelles only granules, while another region of the same parasite cell has few or no appendages and myofibrils are present (Fig. 5, 26).

**PCR.** Using PCR, *Nosema algerae* primers produced no band from the biopsy material utilizing 1, 5, 10  $\mu\text{l}$  of extract at either 48, 50 or 55° C. However, *Nosema algerae* spore extracts amplified under all of these conditions and a strong band at 190-bp was evident using 1  $\mu\text{l}$  of extract. Attempts to amplify *Nosema algerae* spores with conserved primer pairs such as V1(ss18f)::ss1492r or ss530f::ls580r [29] did not yield bands, nor did these primers amplify the biopsy material.

## DISCUSSION

This microsporidian parasite was observed in muscle biopsy tissue. No other opportunistic infections were evident at the time of presentation or in the biopsy. Observations by light

←  
dense exospore coat (Ex) appears to be relatively uniform in density and thickness in this sporoblast, the polar filament (Pf) forms two rows around the periphery of the sporoplasm. Note the presence of large accumulations of vesiculotubular structures (T). 11. Mature spore containing a fully developed electron-lucent endospore coat (average thickness 90–100 nm). The exospore (62 nm) surface has several vesiculotubular structures (T) on it. Note the presence of nine polar filament (Pf) cross sections arranged in two rows. Ribosomes (R) appear in a spiral-like array forming rows around the nuclear area (Nu). 12. Spore containing ten polar filament (Pf) cross sections clustered into three rows. The anisofilar nature of the polar filament is visible in figures 11 and 12. 13. Section through a spore revealing the presence of the anterior anchoring disc complex (A) of the polar filament (Pf) and the manubroid (Mpf) portion of it. The cross sections of polar filament coils arranged in a single row is visible. Multiple rows of ribosomes (R) are also present. Note the presence of vesiculotubular material (T).

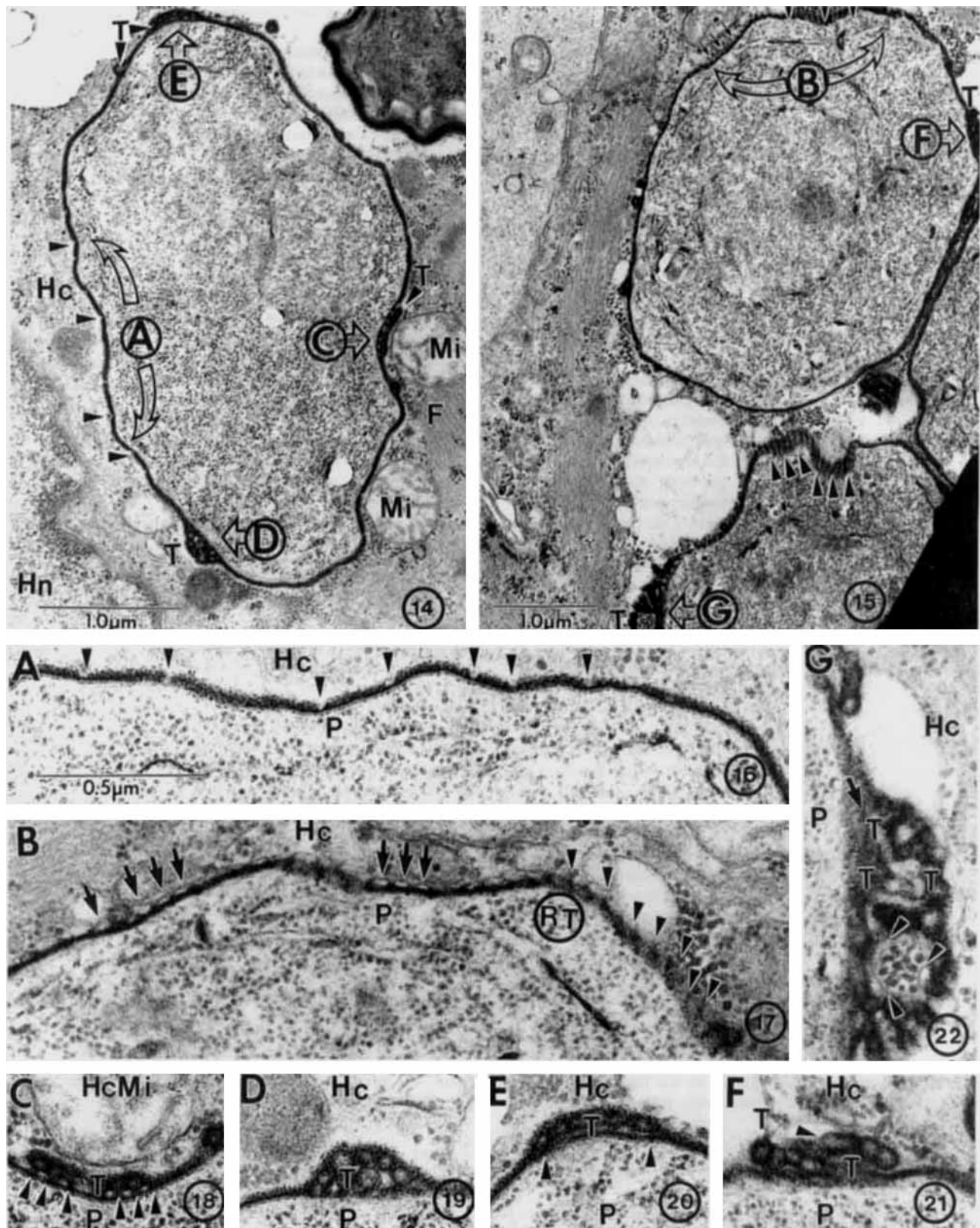


Fig. 14-22. The proliferative cell surface and its secretions (lettered areas A-G on Fig. 14 & 15 correspond to the matching lettered enlargements below). 14. The surface of this proliferative cell consists of uniformly thick electron-dense secretions, with small indentations (arrowheads) down to the cell membrane at irregular intervals and along this surface, occasional vesiculotubular (T) clusters of varying size and complexity are present. The parasite cell is in direct contact with the host cytoplasm (Hc) indicated by the presence of myofilaments (F), mitochondria (Mi), and a host nucleus (Hn). 15. The surface of some proliferative cells vary considerably. In some areas they appear as described previously (Fig. 14) and in other areas they appear to have electron-lucent "blisters" overlying the membrane (arrows). When cut tangentially, the "blistered"

microscopy demonstrated organisms in the myocytes. The organisms were present only in skeletal muscle cell cytoplasm. The surrounding connective tissue and inflammatory cells were uninfected. Upon identification of a microsporidian infection, the patient was treated with albendazole. It alone has efficacy and the combination of albendazole and itraconazole cleared the infection both clinically and histologically. Consequently, the second biopsy of the left quadriceps muscle provided the tissue for all the observations.

Electron microscopic observations confirm that the parasite cells are in direct contact with the muscle cell cytoplasm. The parasite developmental stages observed, contain nuclei in diplokaryon arrangement and they occur as one to two pairs per cell. More than two diplokarya were never observed in one parasite cell thus all proliferation is by binary fission. Since this was the only division process observed, this organism is diploplastic. These features are consistent with the Nosematidae.

All developmental stages observed have electron-dense secretions on the surface of their plasmalemma. This suggests two possibilities; that only sporogony was observed or that the commencement of plasmalemmal thickening (typically indicating the beginning of sporogony in most *Nosema* species) can not be used for this organism [5]. A review of the Nosematidae species indicates that a thickened plasmalemma on early developmental stages, has been demonstrated in two organisms. Avery & Anthony [2], experimentally infected and ultrastructurally studied early development of *N. algerae* in *Anopheles* mosquitoes. Their studies revealed the presence of parasite cells with a thickened plasmalemma from the sporoplasm stage (one hour post exposure) and continuing through all developmental stages. Canning & Sinden [8] and Vavra & Undeen [28] also demonstrated these features, while not having the timing sequence to indicate that the stages were indeed very early. Brooks et al. [4] presented similar findings with *N. varivestis* (transferred to the genus *Annecalia* in 1993 [12]) in another insect host and we believe the human parasite presented in this report, is the third such organism following this developmental pattern. Due to the precocious plasmalemmal thickening, the cytoplasmic density of the parasite cells is used as an alternative developmental indicator for proliferative vs. sporogonic development.

The appendages associated with the surface of this human microsporidian, are most similar to the Type II tubules of Takvorian and Cali [24]. They were described from *Glugea ste-*

*phani* sporonts, measure 25–35 nm in diameter, of greatly varying lengths (1,000–1,600 nm), and are located within the sporogony vacuoles. They occur in tufts and twisted clusters of tubes in cable-like appearance. At high magnification, the individual tubules appear to dilate and contract "like beads on a string." Brooks et al. also related the tubules of *A. varivestis* to the Type II tubules with comments on some differences [4].

The vesiculotubular appendages observed in the current study also have the dilated and contracted appearance along their length and may occur in clusters, however, they are larger in diameter (40–65 nm) and shorter in length (with a maximum observed length of 850 nm). Although clusters are formed, the tubules of this parasite are irregularly arranged with no apparent pattern. Additionally, these tubules secrete and are surrounded by extremely electron-dense material associated with them. This material is fibrous or glycocalyx-like and varies from a thick layer to totally surrounding tubule clusters in large masses. The accumulation of extracellular material may be so dense as to almost obliterate the appearance of the tubules contained in them (Fig. 18–24). However, transparent vesicle-like structures appear throughout the clusters and close examination of them indicates the presence of small electron-transparent centers. The electron-dense secretions surround but do not separate them from the parasite cell surface.

We have called the tubules, vesiculotubular structures because of their extreme dilations and constrictions (Fig. 18–29) often resulting in the appearance of round vesicles. This is clearly demonstrated by the higher magnification micrographs of the proliferative cell surface (Fig. 18–22). In addition to the above mentioned morphological differences, the tubules described in the present study are in association with both proliferative and sporogonic stages and occur on a microsporidium developing in direct contact with host cell cytoplasm. While this is unusual, it may be that the unusual presence of the secretions on the surface in early development is what necessitates the formation of the tubular appendages for nutrient absorption. It should be noted, that they also occur on the surface of the two previously mentioned organisms that develop the precocious thickened plasmalemma (*N. algerae* and *A. varivestis*) on early developmental stages.

Probably the most interesting feature of this microsporidium is the presence of protoplasmic extensions. We are calling these structures protoplasmic extensions because unlike appendages which occur attached to the plasmalemma or emanating from it, these are continuous with the cell cytoplasm and extend from

surface appears ridged or as alternating dark and light bands (arrowheads). In still other areas, the surface has vesiculotubular (T) clusters on it. 16. The fibrous nature of the thick electron-dense secretory material is visible at this magnification. While its thickness seems relatively uniform, irregularly spaced gaps or discontinuities (arrowheads) are present along the parasite (P) plasmalemmal surface.  $\times 62,000$ . 17. Higher magnification of the electron-lucent "blisters" (arrows). The electron-lucent space under the thin coating, in conjunction with the electron-dense protrusions gives the appearance of "blistering." The tangential cut through the transitional region of the plasmalemma surface on the right side (RT) demonstrates the appearance of regular occurring ridges (arrowheads).  $\times 62,000$ . 18–22. Enlargements of five different vesiculotubular complexes surrounded by the fibrous electron-dense glycocalyx-like matrix on the surface of the parasite cells demonstrating the variations of their appearance. Magnification  $\times 62,000$ . Parasite (P), Host cytoplasm (Hc), Host cytoplasmic mitochondrion (HcMi), vesiculotubular structures (T). 18. A vesiculotubular (T) structure lying parallel to the parasite (P) surface and appearing to be attached to it at multiple sites (arrowheads). This area of the plasmalemma is invaginated and adjacent to a host cytoplasmic mitochondrion (HeMi). The vesiculotubular structures and the fibrous matrix which encapsulates them is 400 nm long and 72 nm in height. 19. A cluster of vesiculotubular (T) structures on the parasite (P) surface protruding 160 nm into the host cytoplasmic area (Hc). 20. A vesiculotubular (T) structure lying parallel to a portion of parasite (P) surface and protruding 80–95 nm into the host cytoplasmic area (Hc), appearing to be attached only at the ends (arrows). 21. Three vesiculotubular (T) structures are each attached at one end to the parasite (P) surface with the other ends extending into the host cytoplasm (Hc). The tubular nature of these structures is most apparent in the right one (arrow) which appears to have constrictions and dilations giving it a more tubular appearance. 22. A cluster of vesiculotubular (T) structures emanating from the parasite (P) into the host cytoplasmic area (Hc). The tubular nature of these structures is apparent, they may branch, are extensive, and are covered with the fibrous electron-dense glycocalyx-like substance. Some tubules appear to be continuous with the parasite cell cytoplasm. Additionally, a cluster of structures appearing to be composed of solid electron-dense material in an electron-lucent matrix and limited by a thin envelope (arrowheads) appears amid the tubular cluster, its significance is unknown.

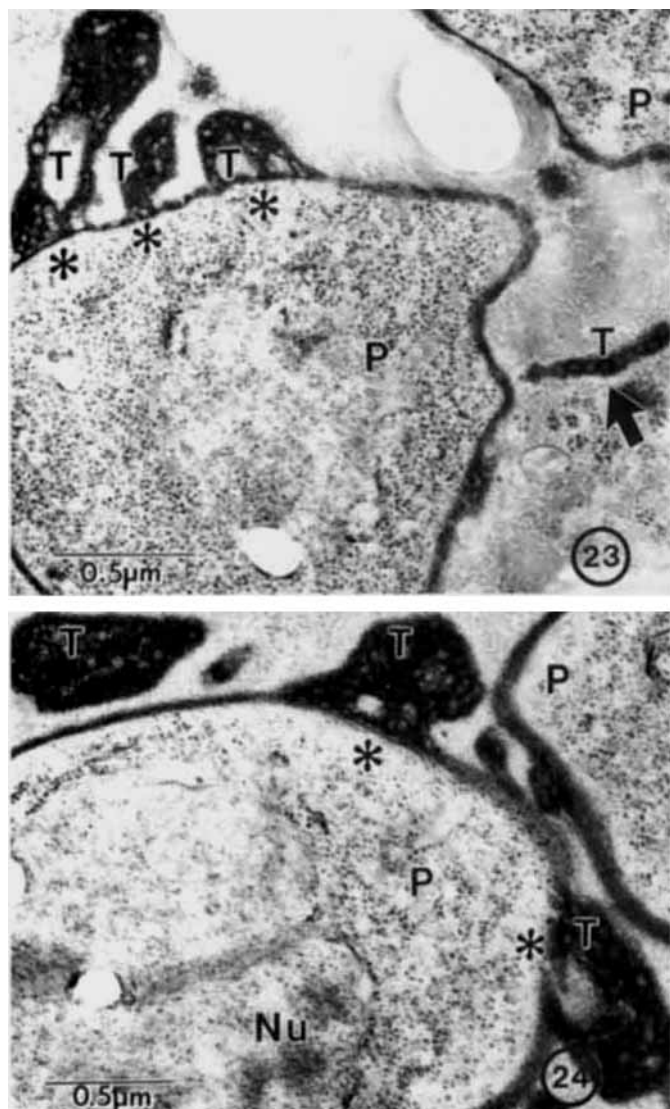


**Fig. 23, 24.** Vesiculotubular complexes. **23.** A parasite cell (P) with large, irregular accumulations of the fibrous and vesiculotubular material (T) extensively protruding off of small areas of the parasite cell surface (\*). These projections extend into the host cytoplasm for more than a micrometer in length while attached to about 0.4  $\mu\text{m}$  of the parasite cell surface. These projections vary from a single vesiculotubular extension (arrow) 0.85  $\mu\text{m}$  in length, to complex clusters. Regardless of their arrangement, the vesiculotubular structures are always within an electron-dense fibrous matrix. **24.** Two parasite cells (P) with accumulations of fibrous and vesiculotubular (T) material protruding off of their cell surfaces. These protrusions extend into the host cell cytoplasmic area from several sites on the membrane. Additional secretions can be seen near one cell, but not attached.

**Fig. 25-29.** Proliferative cells with protoplasmic extensions. **25.** A parasite cell, probably a precursor to an elongated "protoplasmic extension" producing cell. A vesiculotubular "cap" complex (TvC) is well formed on one end and is apparent on the opposite end. Several channels (arrowheads) are visible in the thick surface coat. Note the presence of vesiculotubular (T) structures in the host cytoplasm and myofilaments (F). **26.** This very elongated cell (7.1  $\mu\text{m}$  in length and varies between 1.0 and 1.2  $\mu\text{m}$  wide) possesses the same vesiculotubular "cap" complex (TvC) at one end which relates it to the "transitional" cell and has the scalloped thick plasmalemmal surface which contains several channels (arrowheads). Additionally, this cell possess several protoplasmic extensions (E) of varying lengths, projecting from the cell surface (broad arrows). At the ends of these protoplasmic extensions are vesiculotubular (T) structures with the electron-dense fibrous coating, as previously seen, illustrated on typical proliferative cells. Note the presence of vesiculotubular (T) structures and myofilaments (F) in the host cytoplasm. **27.** A portion of a parasite cell protoplasmic extension complex measuring 4.8  $\mu\text{m}$  in length and between 0.5  $\mu\text{m}$  to less than 0.3  $\mu\text{m}$  in width. A number of branches of varying lengths, have formed from the cell surface and project into the host cytoplasm. These projections also end in vesiculotubular (T) structures with the electron-dense fibrous coating. The cell surface also has some scalloping and shallow indentations present. In the lower third

the cell like arms (Fig. 26-29). Transitional cells between typical developmental forms and the protoplasmic extension cells appear "polarized." That is, they become long and narrow with large vesiculotubular "cap" complex(es) at the end(s) of the long axis. These complexes are maintained on both the transitional and the elongated cells (Fig. 28, 29). It is because of the presence of this complex, that the relationship between these two cell types becomes evident. Although these cells have become greatly elongated they continue to resemble the original proliferative microsporidian cell (Fig. 25).

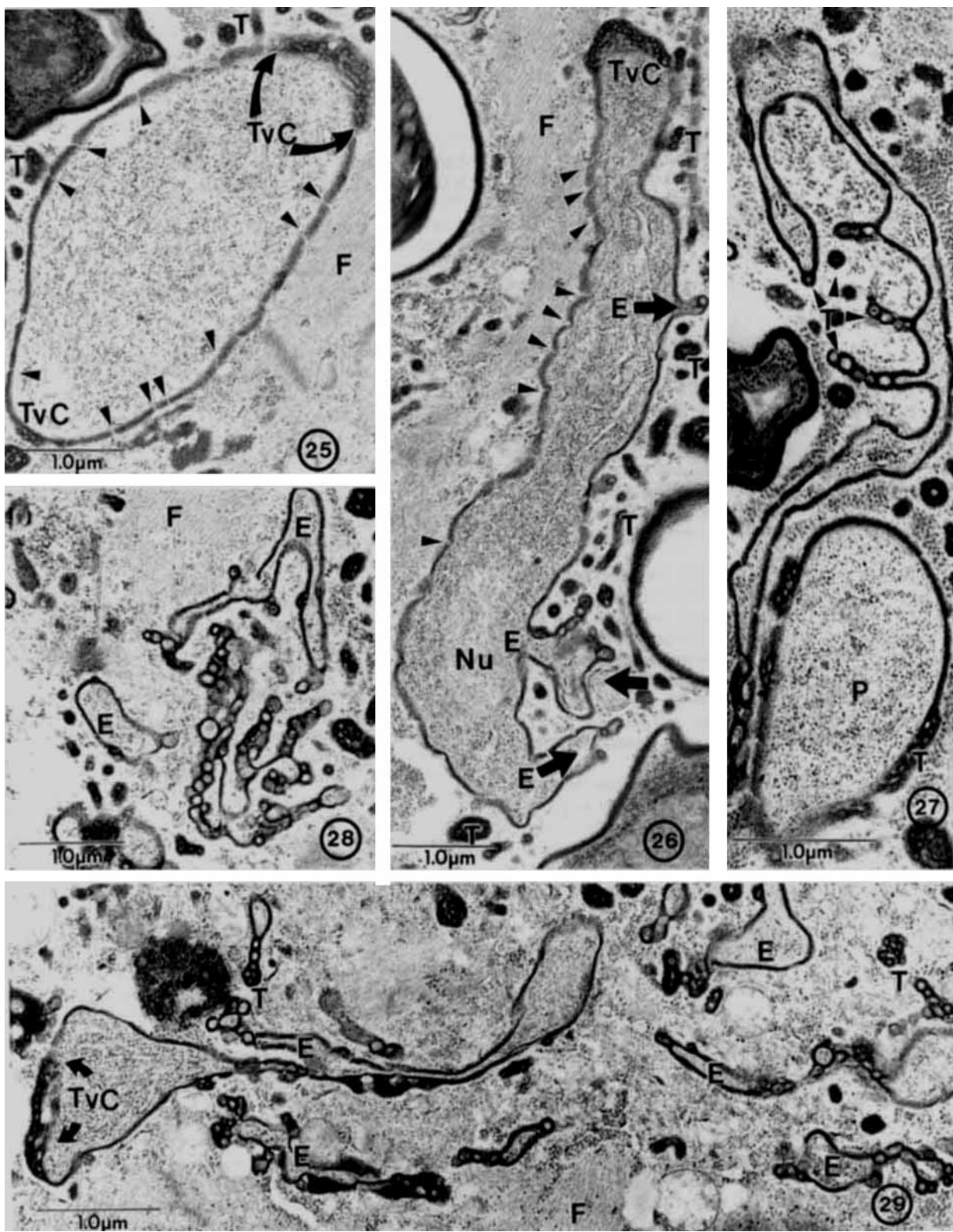
The protoplasmic extensions may branch and vary greatly in both length and width. At the ends of the protoplasmic extensions, vesiculotubular structures develop that are the same as those previously described in association with the surface of the other developing stages. We believe the development of protoplasmic extensions are associated with proliferative development and that they detach during sporogony as do many of the vesiculotubular structures.

It is interesting to note that the only other similar structures observed in the literature are found in mycological reports. They revealed the presence of "biotrophic" fungi, defined as obligate parasites in living cells. These fungi produce branches which obtain nutrients from the host cells without killing them [1].

**Taxonomic considerations.** The basic developmental features of this organism appear most similar to those of the family Nosematidae. In a current Microsporidian taxonomic scheme (1992), three genera were placed in this family, *Nosema bombycis* Naegeli, 1857; *Issia trichopterae* (Weiser, 1946), Weiser, 1977; and *Hirsutusporos austrosimulii* Batson, 1983 [21]. Subsequently, a new genus, *Anncalia meligethi* (Issi & Raditscheva, 1979) Issi, Krylova & Nicolaeva, 1993 was established for *N. meligethi* with *N. varivestis* added as a second species and also placed in this genus [12]. Of these genera, *Nosema* and *Anncalia* are the most similar but neither are thermophilic with the exception of *Nosema connori* and possibly *N. ocularum* and *N. algerae*.

**Temperature considerations.** The patient in the present study presented with fever (38° C) and the tissue biopsied was from deep muscle (quadriceps). The micrographs clearly indicate that the parasite was proliferating and producing spores at this temperature.

*Nosema algerae*, a parasite of mosquitoes, has been shown to grow in temperatures ranging from 26° C to 35° C in several kinds of tissue cultures including insects of many families, amphibians, and several mammalian cell lines [19, 27] and we have grown them in rabbit kidney cells (A. C. & P. M. T., unpubl. data). However, at 37° C Undeen reported infection that lasted only three days with no spore production and observed no infection at 38° C [27]. Recently, Trammer et al. [26] commenting about temperature limitations stated: "Considering that *N. algerae* failed to proliferate in cell culture at 37° C [19, 27] and that *N. algerae* was observed in this study only in the



of the figure is a section of a parasite (P) cell with several vesiculotubular (T) structures attached to the cell surface. 28. Several vesiculotubular structures attached to protoplasmic extensions (E). 29. An elongated protoplasmic extension, continuous with a portion of the parasite cell and vesiculotubular "cap" complex (TvC). This portion of the cell is more than 5.5  $\mu\text{m}$  long and varies from 1.3  $\mu\text{m}$  wide at its cap end to less than 0.5  $\mu\text{m}$  at the opposite end. The narrow isthmus between the two ends of the cell is only 0.1  $\mu\text{m}$  wide. Another protoplasmic extension (E) branches from the surface (0.8  $\mu\text{m}$ ) and terminates in a vesiculotubular (T) complex, covered with the electron-dense coat. Note the numerous clusters of protoplasmic extensions (E) terminating in vesiculotubular structures throughout this host cell cytoplasm and the lack of organized myofilaments in the vicinity of the protoplasmic extensions.

extremities of athymic mice, we assume both immunodeficiency and lower temperature are necessary for *N. algerae* to proliferate in mice." Thus indicating a physiological difference between the human parasite in this study and *N. algerae*.

Additionally, *N. algerae* has been shown to disseminate to every tissue type in both insects [19, 27] and the athymic mouse tail from the above study [26]. The parasite in the current study has been found only in the skeletal muscle. The biopsy tissue samples contained other tissues but none were infected. *Nosema algerae* spores contain polar filament coils arranged in a single row in all publications including; its growth in its type host [28], various types of tissue culture from invertebrate and vertebrate hosts [23] and its growth at various temperatures [19, 27]. The parasite in the current study typically contains a polar filament arranged in two rows of coils and occasionally one or three rows and it is anisofilar (Fig. 11-13).

*Nosema bombycis* Naegeli, 1857 is the type species for the genus *Nosema*. It is not known to have appendages or protoplasmic extensions and its plasmalemmal thickening occurs at the onset of sporogony. Appendages occur on many microsporidia and have been given variable taxonomic significance. In some cases they have been the subject of the genus establishment e.g. *Loma* [15] and *Hirsutusporos* [21], in others they have been considered species features e.g. *Glugea stephani* [24]. While precocious plasmalemmal thickening is atypical, it occurs on *N. algerae* [2] and *A. varivestis* [4], as yet it has not been given taxonomic significance.

The only species still in *Nosema* that possesses tubular appendages and a thickened plasmalemma throughout its development is *N. algerae* and it has been suggested that it too should be moved. Baker et al. [3], studied phylogenetic relationships among *Vairimorpha* and *Nosema* species based on ribosomal RNA sequence data, and stated: "Our results indicate that once a broader range of microsporidian genera have been studied, a number of *Nosema* species including *N. kingi*, *N. algerae*, and *N. locustae*, will need new taxonomic designations."

The PCR results in the present study indicate that the primers used to successfully amplify *N. algerae* could not amplify the human organism. While the taxonomic placement of *N. algerae* is beyond the scope of this paper, and possibly the subject of another publication, its elimination from consideration, as regard to the parasite of this study, is based on morphological, genetic, and physiological features.

**Comparison with other diplokaryotic human infecting microsporidia.** *Nosema connori*, Sprague, 1974 [20], is a disseminated organism that caused malabsorption diarrhea in an athymic infant with a temperature of 38.5° C [14]. Its spores are  $4 \times 2 \mu\text{m}$  with 10–12 polar filament coils arranged in a single row. Most of the autopsy tissues examined were infected, including epithelial, connective, and muscle tissue [22]. While this organism does infect skeletal muscle, it also infects all other tissue types and produces a larger spore. Additionally, it should be noted that micrographs of *N. connori*, in previously published papers, contained structures that were either unlabeled [16] or mislabeled as extruded polar tubules [14] and they are, in actuality, very similar to our vesiculotubular structures. It is probable that the *Nosema*-like organisms that readily grow at warm blooded host temperatures, are a group. They share significant physiological differences from the true *Nosema* species that grow at lower temperatures, in invertebrates. At this time we propose the removal of *N. connori* from the genus *Nosema*, placing it as a second species in the new genus.

*Nosema ocularum* Cali et al., 1991 is an organism associated with corneal ulceration. It is characterized by the presence of large,  $3 \times 5 \mu\text{m}$  diplokaryotic spores containing 9–12 polar

filament coils arranged in a single row [7]. It lacks all of the unique features which are characteristic of the organism in the present study and only grew in the outer layers of the corneal stroma.

*Nosema corneum* now *Vittaforma corneae* (Shadduck et al., 1990) Silveira and Canning, 1995, was removed from the genus *Nosema* and family Nosematidae because of features not originally observed including tetra or octosporoblastic sporogony which also eliminates *Vittaforma* from consideration here [17, 18].

It should also be noted that since both *Nosema ocularum* and *Vittaforma corneae* are organisms only observed in the eye, it, like the mouse tail and foot pads (where *N. algerae* growth was observed), may maintain a slightly lower temperature consequently, they should not be considered as a part of what we have defined as a "thermophilic" group.

Other than *Nosema*, the genera of the Nosematidae are based on the presence of dimorphism or tubular appendages while maintaining the basic life cycle characteristics. Similarly, the organism described in this report, maintains the basic life cycle characteristics and includes a new type of vesiculotubular appendages. Additionally, it possesses unique protoplasmic extensions and grows at 37–38° C. No other established genus has the unique combination of characteristics exhibited by the organism in the present study, consequently, it is placed in a new genus, in the family Nosematidae.

**Taxonomic summary.** *Brachiola* n. g. Thermophilic, proliferating and sporulating at temperatures  $\geq 37^\circ \text{C}$ . Nuclei are in diplokaryotic arrangement throughout the life cycle. Multiplication is by simple fission of elongated cells, no plasmodial stages develop. Parasite stages are in direct contact with the host cell cytoplasm. All stages are covered with electron-dense secretions (precocious thickened plasmalemma) and a variety of plasmalemmal ornamentations including various forms of appendages which may be on the cell surface or attached to protoplasmic extensions. These structures may dissociate from the parasite cell surface during sporogony, resulting in fewer of them on the spores. Development is sporoblastic, thus, sporeonts produce two diplokaryotic spores.

*Brachiola vesicularum*, n. sp. The features of the genus. The cytokinetic and karyokinetic processes are linked, resulting in no more than two diplokarya per cell and binary fission as the means of replication. All stages possess secretions on the plasmalemma producing the "thickened" membrane appearance. These stages are characterized by a variety of plasmalemmal ornamentations, including "blisters", ridges, and vesiculotubular appendages with accompanying electron-dense secretions or surface coverings. Some vesiculotubular appendages are attached to protoplasmic extensions projecting from the parasite cells. The protoplasmic extensions of these cells extend into the surrounding host cytoplasm and may be branched. In sporogony, the plasmalemmal covering becomes more uniformly dense and thicker. The vesiculotubular appendages are still present but embedded in a matrix which has increased in electron-density, and protrudes greater distances from the plasmalemma. Each sporeont produces two diplokaryotic sporoblasts which become more electron-dense, crenated and may still have some vesiculotubular material attached through mature spore formation. The formalin fixed spores are  $2.5\text{--}2.9 \times 1.9\text{--}2.0 \mu\text{m}$  (usually  $2.9 \times 2.0 \mu\text{m}$ ) and contain 7–10 coils of the polar filament, usually nine arranged in two rows but may also occur in one or three rows. While the arrangement of the polar filament coils vary, the number of coils is relatively constant and the last two to three coils are smaller in diameter, thus the polar filament is anisofilar and no spore dimorphism is reported. The

development is asynchronous, i.e. multiple stages occur within a cluster.

*Brachiola vesicularum*, n. g., n. sp.  
A. Cali, P.M. Takvorian, & L. M. Weiss

**Type host.** *Homo sapiens*

**Site of infection.** Striated muscle tissue.

**Development.** As for the genus and species.

*Brachiola connori* (Sprague 1974) n. comb.  
A. Cali, P.M. Takvorian, & L. M. Weiss

**Synonymy.** *Nosema connori* Sprague 1974 [20].

The generic name, *Brachiola*, reflects one of the features of the organism. *Brachiola*, Latin for little arms or extensions, referring to the protoplasmic extensions and *vesicularum* from the Latin *vesicula* meaning little pouch or vessel, for the vesiculotubular appendages.

#### ACKNOWLEDGMENTS

The authors wish to thank Jason Retig of Beth Israel Medical Center, Pathology Dept., NYC for his assistance with the preparation of the tissues biopsied for this study, and Mario Constantino, chairman foreign languages, Tottenville High School, NYC for assistance with Latin terminology. Supported by NIH Grant A131788.

#### LITERATURE CITED

- Alexopoulos, C. J., Mims, C. W., & Blackwell, M. 1996. Introductory Mycology. John Wiley & Sons, Inc. New York. Pp. 868.
- Avery, S. W. & Anthony D. W. 1983. Ultrastructural study of early development of *Nosema algerae* in *Anopheles albimanus*. *J. Invert. Pathol.*, **42**:87–95.
- Baker, M. D., Vossbrinck, C. R., Maddox, J. V., & Undeen, A. H. 1994. Phylogenetic relationships among *Vairimorpha* and *Nosema* species (Microspora) based on ribosomal RNA sequence data. *J. Invert. Pathol.*, **64**:100–106.
- Brooks, W. M., Hazard, E. I., & Bechnel, J. 1985. Two new species of *Nosema* from the Mexican bean beetle, *Epilachna varivestis*. *J. Protozool.*, **32**:525–535.
- Cali, A., 1971. Morphogenesis in the genus *Nosema*. Proc. IV Intl. Colloq. Insect Pathol., College Park, MD, 1970. Pp. 431–438.
- Cali, A., Orenstein, J. M. & Kottler, D. 1993. *Septata intestinalis*, n. g., n. sp., an intestinal microsporidian associated with chronic diarrhea and dissemination in AIDS patients. *J. Euk. Microbiol.*, **40**:101–112.
- Cali, A., Meisler, D. M., Lowder, C. Y., Lembach, R., Ayers, L., Takvorian, P. M., Rutherford, I., Longworth, D. L., McMahon, J. T. & Bryan, R. T. 1991. Corneal microsporidioses: characterization and identification. *J. Protozool.*, **38**:215S–217S.
- Canning, E. U. & Sinden, R. E. 1973. Ultrastructural observations on the development of *Nosema algerae* Vavra and Undeen (Microspora, Nosematidae) in the mosquito *Anopheles stephensi* Liston. *Protistologica*, **9**:405–415.
- Chupp, G. L., Alroy, J., Adelman, L. S., Breen, J. C. & Skolnik, P. R. 1993. Myositis due to *Pleistophora* in a patient with AIDS. *Clinical Infectious Diseases*, **16**:15–21.
- Desportes, I., Le Charpentier, Y., Galian, A., Bernard, F., Co- chand-Priollet, B., Lavergne, A., Ravisse, P. & Modigliani, R. 1985. Occurrence of a new microsporidian: *Enterocytozoon bieneusi* n. g., n. sp. in the enterocytes of a human patient with AIDS. *J. Protozool.*, **32**: 250–254.
- Hollister, W. S., Canning, E. U., Weidner, E., Field, A. S., Kench, J., & Marriott, D. J. 1996. Development and ultrastructure of *Trachipleistophora hominis* n. g., n. sp. after in vitro isolation from an AIDS patient and inoculation into athymic mice. *Parasitology*, **112**:143–154.
- Issi, I. V., Krylova, S. V., & Nicolaeva, V. M.. 1993. The ultrastructure of the microsporidium *Nosema meligethi* and establishment of the new genus *Annocalia*. *Parazitologiya*, **27**:127–133.
- Ledford, D. K., Overman, M., Gonzalvo, A., Cali, A. & Lockey, R. F. 1985. Microsporidiosis myositis in the acquired immune deficiency syndrome. *Ann. Internal Med.*, **102**:628–630.
- Margileth, A. M., Strano, A. J., Chadra, R., Neafie, R., Blum, M. & McCully, R. M. 1973. Disseminated nosematosis in an immunologically compromised infant. *Arch. Pathol.*, **95**:145–150.
- Morrison, C. M. & Sprague, V. 1981. Electron microscopical study of a new genus and new species of microsporidia in the gills of Atlantic Cod *Gadus morhua* L. *J. Fish Dis.*, **4**:15–32.
- Shadduck, J. A., Kelsoe, G. & Helmke, R. J. 1979. A microsporidan contaminant of a nonhuman primate cell culture: ultrastructural comparison with *Nosema connori*. *J. Parasitol.*, **65**:185–188.
- Shadduck, J. A., Meccoli, R. A., Davis, R. & Font, R. 1990. Isolation of a microsporidian from a human patient. *J. Infect. Disease.*, **162**:773–776.
- Silveira, H. & Canning, E. U. 1995. *Vittaforma corneae* n. comb. = for the human microsporidium *Nosema corneum* Shadduck, Meccoli, Davis & Font. 1990, based on its ultrastructure in the liver of experimentally infected athymic mice. *J. Euk. Microbiol.*, **42**:158–165.
- Smith, J. E., Barker, R. J., & Lai, P. F. 1982. Culture of microsporidia from invertebrates in vertebrate cells. *Parasitol.*, **85**:427–435.
- Sprague, V. 1974. *Nosema connori* n. sp., a microsporidian parasite of man. *Trans. Am. Microsc. Soc.*, **93**:400–403.
- Sprague, V., Bechnel, J. J. & Hazard, E. I. 1992. Taxonomy of Phylum Microspora. *Crit. Rev. Microbiol.*, **18**:285–395.
- Strano, A. J., Cali, A. & Neafie, R. C. 1976. Microsporidiosis In: Binford, C. H. & Connor, D. H. (ed.), Pathology of Tropical and Extraordinary Diseases, An Atlas, Volume One, Armed Forces Institute of Pathology Press. **14**:336–339.
- Streett, D. A., Ralph, D., & Hink, W.F. 1980. Replication of *Nosema algerae* in three insect cell lines. *J. Protozool.*, **27**:113–117.
- Takvorian, P. M. & Cali, A. 1983. Appendages associated with *Glugea stephani* a microsporidan found in flounder. *J. Protozool.*, **30**: 251–256.
- Terada, S., Reddy, R., Jeffers, L. J., Cali, A., & Schiff, E. R. 1987. Microsporidan hepatitis in a patient with the Acquired Immunodeficiency Syndrome. *Ann. Internal Med.*, **107**:61–62.
- Trammer, T., Dombrowski, F., Doehring, M., Maier, W. A. & Seitz, H. M. 1997. Opportunistic properties of *Nosema algerae* (Microspora), a mosquito parasite, in immunocompromised mice. *J. Euk. Microbiol.*, **44**:258–262.
- Undeen, A. H. 1975. Growth of *Nosema algerae* in pig kidney cell cultures. *J. Protozool.*, **22**:107–110.
- Vavra, J. & Undeen, A. H. 1970. *Nosema algerae* n. sp. a pathogen in a laboratory colony of *Anopheles stephensi* Liston. *J. Protozool.*, **17**:240–249.
- Weiss L. M. & Vossbrinck, C. R. 1998. Microsporidiosis: molecular and diagnostic aspects. *Adv. Parasitol.*, in press.

Received 6-18-97, 12-17-97; accepted 12-31-97